Inorg. Chem. **2009**, *48*, 2976−2984

Aqueous Coordination Chemistry of H_2: Why is Coordinated H_2 Inert to Substitution by Water in *trans*-$Ru(P_2)_2(H_2)H^+$-type Complexes (P_2 = a Chelating Phosphine)?

Nathaniel K. Szymczak, Dale A. Braden, Justin L. Crossland, Yevgeniya Turov, Lev N. Zakharov, and David R. Tyler*

Department of Chemistry, University of Oregon, Eugene, Oregon 97403

Received October 3, 2008

The reactivity of a series of *trans*-$Ru(P_2)_2Cl_2$ complexes with H_2 was explored. The complexes reacted with H_2 via a stepwise H_2 addition/heterolysis pathway to form the *trans*-$[Ru(P_2)_2(H_2)H]^+$ dihydrogen complexes. Some of the resulting η^2-H_2 complexes were surprisingly inert to substitution by water, even at concentrations as high as 55 M; however, the identity of the bidentate phosphine ligand greatly influenced the lability of the coordinated η^2-H_2 ligand. With less electron-donating phosphine ligands, the H_2 ligand was susceptible to substitution by H_2O, whereas with more electron-rich phosphine ligands, the H_2 ligand was *inert* to substitution by water. Density functional theory (DFT) calculations of the ligand substitution reactions showed that the Ru−H_2 and Ru−H_2O complexes are very close in energy, and therefore slight changes in the donor properties of the bidentate phosphine ligand can inhibit or promote the substitution of H_2O for H_2.

Introduction

The coordination chemistry of dihydrogen is gaining increased awareness as a result of the recent movement toward a hydrogen economy.[1] To sustain such an economy, a thorough understanding of how dihydrogen can be produced and how it interacts with its surroundings on a molecular level is needed. A particularly attractive route for H_2 generation is inspired by biology. The hydrogenase enzymes mediate the conversion of protons and electrons to H_2 with impressive efficiency.[2] One approach that has been explored extensively to exploit this function is the construction of synthetic models of the active site of Fe−Fe and Fe−Ni hydrogenase enzymes with the goal of synthesizing a viable catalyst for H_2 production.[3−6] Such models replicate key structural features found in the enzyme active site, and for the H-cluster (the most widely modeled site), this involves a binuclear iron core featuring three CO ligands, two CN^{-1} ligands, and a thiolate bridging from the Fe_4S_4 cluster.[7,8] Another noteworthy class of molecules that replicate the proposed aza-dithiolate linkage of the H-cluster are described by Dubois and co-workers.[9] Nickel phosphine complexes that incorporate pendant amine bases in their periphery were shown to act as functional hydrogenase mimics, and such reactivity was proposed to result from the delivery of exogenous protons through the proton relay system.

From a mechanistic standpoint, the intermediates involved in conversion of H^+ to H_2 are unusual. Although several pathways have been proposed, a common feature is the presence of a coordinated hydride and a coordinated H_2 ligand at biological conditions, namely in water (Figure 1).[5]

An unusual feature of the mechanism is the competitive ability of water, H_2, and hydrides to coordinate to an iron center.[10] This unique ability of hydrogenase enzymes and related biomimics was recently highlighted for a heterobi-

* To whom correspondence should be addressed. E-mail: dtyler@uoregon.edu.

(1) Kubas, G. J. *Chem. Rev.* **2007**, *107*, 4152–4205.
(2) Frey, M. *ChemBioChem* **2002**, *3*, 153–160.
(3) Darensbourg, M. Y.; Lyon, E. J.; Smee, J. J. *Coord. Chem. Rev.* **2000**, *206−207*, 533–561.
(4) Darensbourg, M. Y.; Lyon, E. J.; Zhao, X.; Georgakaki, I. P. *Proc. Natl. Acad. Sci. U.S.A.* **2003**, *100*, 3683–3688.
(5) Georgakaki, I. P.; Darensbourg, M. Y. *Compr. Coord. Chem. II* **2004**, *8*, 549–568.
(6) Linck, R. C.; Rauchfuss, T. B. In *Bioorganometallics: Biomolecules, Labeling, Medicine*; Jaouen, G., Ed.; Wiley-VCH Verlag GmbH & Co.: Weinheim, 2006; pp 403−435.
(7) Chen, Z.; Lemon, B. J.; Huang, S.; Swartz, D. J.; Peters, J. W.; Bagley, K. A. *Biochemistry* **2002**, *41*, 2036–2043.
(8) Nicolet, Y.; de Lacey, A. L.; Vernede, X.; Fernandez, V. M.; Hatchikian, E. C.; Fontecilla-Camps, J. C. *J. Am. Chem. Soc.* **2001**, *123*, 1596–1601.
(9) Wilson, A. D.; Shoemaker, R. K.; Miedaner, A.; Muckerman, J. T.; DuBois, D. L.; DuBois., M. R. *Proc. Natl. Acad. Sci. U.S.A.* **2007**, *104*, 6951–6956.

10.1021/ic801884x CCC: $40.75
Published on Web 03/02/2009

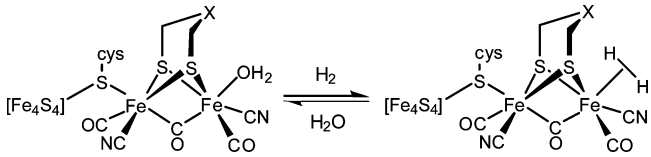

Figure 1. Relevant H_2O/H_2 interconversion scheme with two likely intermediates in the hydrogenase-mediated reduction of protons.

metallic Ni−Ru system, where a Ni(μ-H)Ru complex was formed under ambient conditions by allowing the parent *aqua* complex to react with dihydrogen in water.[11] Given the importance of the H_2 conversion pathway, it is worthwhile to understand some of the underlying reactivity trends associated with this rather elusive class of complexes, namely water-soluble, stable M−(H_2) and M−H complexes.

While the competition between water and H_2 in transition-metal complexes is not completely unprecedented, most studies thus far have been reported in non-aqueous solvents (with water as an immiscible phase, thus lowering the effective concentration), or under high H_2 pressures. For example, Kubas and co-workers showed that at low concentrations of water (in hexanes), H_2 was not displaced by water on a tungsten carbonyl fragment. However, the presence of excess water [in tetrahydrofuran (THF) solution] resulted in substitution of the H_2 ligand.[12] In a related study that highlights similar H_2/H_2O binding enthalpies in non-aqueous solutions on $RuTp(PPh_3)_2^+$ complexes, Lau, Jia, and co-workers found that in dichloromethane solutions water could be displaced by H_2 at elevated pressures (20 atm).[13] Without the excess hydrogen pressure in acidic solution, the H_2 ligand was displaced by H_2O. However, when an excess of water was introduced in dichloromethane solution at a lower pressure of H_2 (10 atm), the substitution reaction was suppressed and instead, deprotonation of coordinated H_2 by H_2O resulted.

We recently reported the generation of several water-soluble η^2-H_2 hydride complexes of iron and ruthenium (eq 1).[14−16] These complexes were formed in water following heterolytic cleavage of an initially coordinated H_2 ligand under moderate conditions.

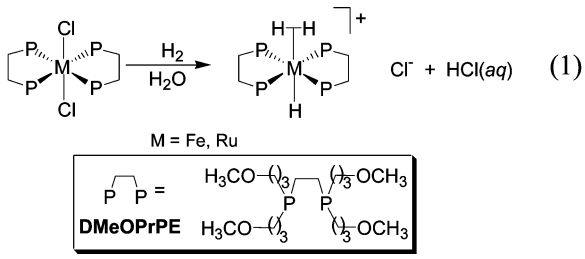

(1)

Several features of this system were unexpected, including the surprising inertness of the coordinated H_2 ligand to substitution by water. Previously, coordination complexes containing an η^2-H_2 were exceedingly rare in aqueous solution,[17,18] particularly without a high pressure of H_2. We have since extended the scope of aqueous coordination chemistry of dihydrogen with the goal of understanding the key factors that allow a coordinated H_2 ligand to be inert to substitution in 55 M water. Herein, we report the results of our study focused on the examination of the reactivity of a variety of ruthenium bidentate phosphine complexes with H_2 in the presence of excess water.

Results

Synthesis of the *trans*-$Ru(P_2)_2Cl_2$ Complexes. The syntheses of complexes **Ia-f** proceeded smoothly with $[Ru(COD)Cl_2]_n$ and the appropriate bidentate phosphine in refluxing ethanol solution using the route previously reported for complex **Ic** (eq 2).

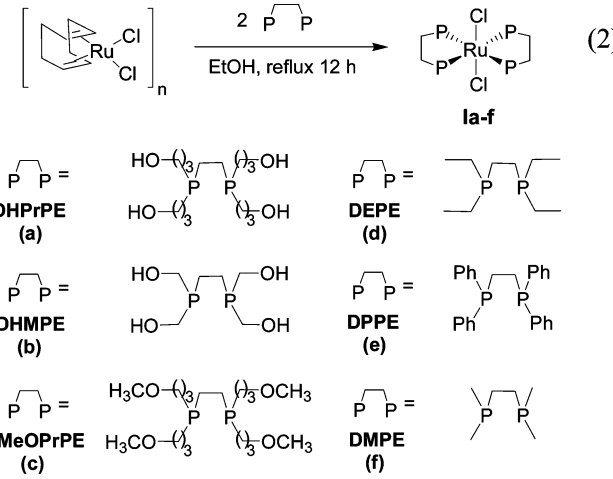

(2)

Complexes **Id**, **Ie**, and **If** were previously synthesized by a slightly different route, and the molecules prepared by the route in eq 2 were spectroscopically identical to the previously reported spectra.[19−21] Solutions containing **I** exhibit a singlet in the $^{31}P\{^1H\}$ NMR spectrum, confirming a *trans* geometry (Table 1). Slow cooling of concentrated solutions of **Ia** and **Ib** resulted in the precipitation of yellow crystals suitable for X-ray crystallographic analysis (Table 2). The structures (Figure 2 and Supporting Information, Figure S1) show an octahedral coordination environment around ruthenium with *trans* chloride ligands. In the case of **Ib**, hydrogen bonds (O−H···Cl) between two hydroxyl groups and the coordinated chloride are present, as shown by the close Cl···O contact (3.03 Å).

(10) Huhmann-Vincent, J.; Scott, B. L.; Kubas, G. J. *Inorg. Chim. Acta* **1999**, *294*, 240–254.

(11) Ogo, S.; Kabe, R.; Uehara, K.; Kure, B.; Nishimura, T.; Menon, S. C.; Harada, R.; Fukuzumi, S.; Higuchi, Y.; Ohhara, T.; Tamada, T.; Kuroki, R. *Science* **2007**, *316*, 585–587.

(12) Kubas, G. J.; Burns, C. J.; Khalsa, G. R. K.; Van Der Sluys, L. S.; Kiss, G.; Hoff, C. D. *Organometallics* **1992**, *11*, 3390–3404.

(13) Chan, W.; Lau, C.; Chen, Y.; Fang, Y.; Ng, S.; Jia, G. *Organometallics* **1997**, *16*, 34–44.

(14) Szymczak, N. K.; Zakharov, L. N.; Tyler, D. R. *J. Am. Chem. Soc.* **2006**, *128*, 15830–15835.

(15) Gilbertson, J. D.; Szymczak, N. K.; Tyler, D. R. *J. Am. Chem. Soc.* **2005**, *127*, 10184–10185.

(16) Gilbertson, J. D.; Szymczak, N. K.; Tyler, D. R. *Inorg. Chem.* **2004**, *43*, 3341–3343.

(17) Li, Z. W.; Taube, H. *J. Am. Chem. Soc.* **1991**, *113*, 8946–8947.

(18) Aebischer, N.; Frey, U.; Merbach, A. E. *Chem. Commun.* **1998**, 2303–2304.

(19) Buys, I. E.; Field, L. D.; George, A. V.; Hambley, T. W.; Purches, G. R. *Aust. J. Chem.* **1995**, *48*, 27–34.

(20) Chang, C.; Ting, P.; Lin, Y.; Lee, G.; Wang, Y. *J. Organomet. Chem.* **1998**, *553*, 417–425.

(21) Clark, S. F.; Petersen, J. D. *Inorg. Chem.* **1983**, *22*, 620–623.

Table 1. Summary of ^{31}P NMR Data for *trans*-$RuCl_2(P_2)_2$ Complexes[a]

complex	$^{31}P\{^1H\}$
$Ru(DHPrPE)_2Cl_2$ (**Ia**)[b]	41.2
$Ru(DHMPE)_2Cl_2$ (**Ib**)[b]	59.8
$Ru(DMeOPrPE)_2Cl_2$ (**Ic**)[14]	44.4
$Ru(DEPE)_2Cl_2$ (**Id**)[19]	48.0
$Ru(DPPE)_2Cl_2$ (**Ie**)[20]	45.8
$Ru(DMPE)_2Cl_2$ (**If**)[21]	37.4

[a] DHPrPE = 1,2-bis(dihydroxypropylphosphino)ethane, DHMPE= 1,2-bis(dihydroxymethylphosphino)ethane, DMeOPrPE= 1,2-bis(dimethoxypropylphosphino)ethane, DEPE= 1,2-bis(diethylphosphino)ethane, DPPE= 1,2-bis(diphenylphosphino)ethane, DMPE= 1,2-bis(dimethylphosphino)ethane. [b] This work.

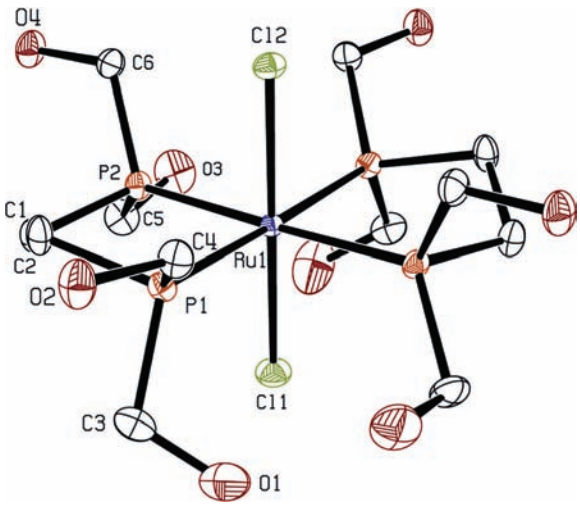

Figure 2. ORTEP representation of *trans*-$Ru(DHMPE)_2Cl_2$ (**Ib**). Ellipsoids are shown at 50% probability. Hydrogen atoms and solvent water molecules are omitted for clarity.

Synthesis of *trans*-$[Ru(P_2)_2H(H_2)]^+$ Complexes. Solutions of **I** are stable in the absence of oxygen, even at elevated temperatures, and ligand substitution reactions did not occur in organic solvents by simply heating **I** in the presence of an incoming ligand. Rather, addition of a strong chloride abstraction reagent is required to produce an open coordination site for binding the H_2 ligand. Complexes **IIa-f** were prepared in toluene or THF with ~350 psig H_2 at 85 °C using $TlPF_6$ as a chloride abstractor and Proton Sponge as a proton sequestering reagent (eq 3).

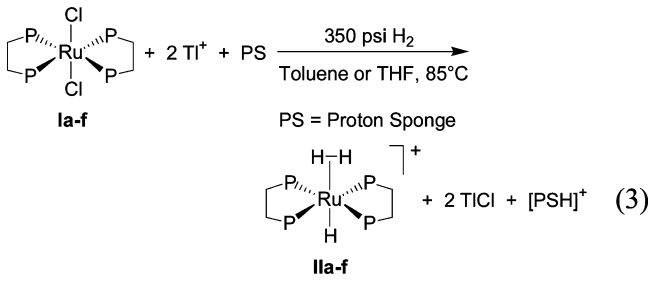

Solutions containing the light-yellow complexes, **IIa-f**, gave rise to a single resonance in the $^{31}P\{^1H\}$ NMR spectrum and displayed ^1H resonances for the η^2-H_2 and hydride ligands as a broad singlet and quintet, respectively (Table 3). The ^1H T_1(min) values of the H_2 resonance were experimentally determined and are also listed in Table 3. All of the determined ^1H T_1(min) values were consistent with a coordinated η^2-H_2 ligand in the short distance regime (0.83 Å−0.86 Å), assuming fast rotation.[22] H/D exchange with methanol-d_4 occurred for the η^2-H_2 ligand over several hours to form the HD isotopologue. From the isotopologue, the $^1J_{HD}$ was determined and an H−H distance was calculated using Morris',[23] Heinekey's[24] and Gusev's[25] relationships. According to the $^1J_{HD}$ values, the H−H bond distances for all the η^2-H_2 complexes are estimated between 0.87 Å−0.91 Å, values well within the short regime of dihydrogen complexes.

Table 2. Crystal Data and Structure Refinement for *trans*-$Ru(DHMPE)_2Cl_2$ (**Ib**)

empirical formula	$C_{12}H_{36}Cl_2O_9P_4Ru$
formula weight	620.26
temperature	153(2) K
wavelength	0.71073 Å
crystal system	monoclinic
space group	*C*2/*c*
unit cell dimensions	a = 10.8376(15) Å b = 24.915(4) Å c = 9.5442(13) Å α = 90° β = 118.651(2)° γ = 90°
volume	2261.6(5) Å^3
Z, Z'	4, 0.5
density (calculated)	1.822 Mg/m^3
absorption coefficient	1.254 mm^{-1}
F(000)	1272
crystal size	0.09 × 0.06 × 0.03 mm^3
theta range for data collection	1.63 to 28.26°
index ranges	$-14 \le h \le 12$, $-33 \le k \le 30$, $-12 \le l \le 12$
reflections collected	9139
independent reflections	2662 [R(int) = 0.0389]
completeness to theta = 28.26°	94.9%
absorption correction	semiempirical from equivalents
max. and min. transmission	1.000 and 0.554
refinement method	full-matrix least-squares on F^2
data/restraints/parameters	2662/0/129
goodness-of-fit on F^2	1.094
final R indices [I > 2sigma(I)]	R1 = 0.0497, wR2 = 0.1251
R indices (all data)	R1 = 0.0662, wR2 = 0.1376
largest diff. peak and hole	2.188 and −0.822 e Å^{-3}

Mechanism for the Formation of *trans*-$[Ru(P_2)_2H(\eta^2\text{-}H_2)]^+$. Following the addition of H_2 to **I**, there are two possible pathways for the formation of **II** (Scheme 1). In the next step, the H_2 can either be heterolytically cleaved by reaction with a base (top path, Scheme 1) or a second H_2-substitution may occur to give a *bis*-η^2-H_2 species (bottom path, Scheme 1). Note that *bis*-η^2-H_2 complexes are uncommon and typically are stabilized by second- and third-row transition metals such as ruthenium or osmium.[28,29]

(22) Morris, R. H. *Coord. Chem. Rev.* **2008**, *252*, 2381–2394.
(23) Maltby, P. A.; Schlaf, M.; Steinbeck, M.; Lough, A. J.; Morris, R. H.; Klooster, W. T.; Koetzle, T. F.; Srivastava, R. C. *J. Am. Chem. Soc.* **1996**, *118*, 5396–5407.
(24) Heinekey, D. M.; Luther, T. A. *Inorg. Chem.* **1996**, *35*, 4396–4399.
(25) Gusev, D. G. *J. Am. Chem. Soc.* **2004**, *126*, 14249–14257.
(26) Bautista, M. T.; Cappellani, E. P.; Drouin, S. D.; Morris, R. H.; Schweitzer, C. T.; Sella, A.; Zubkowski, J. *J. Am. Chem. Soc.* **1991**, *113*, 4876–4887.
(27) Field, L. D.; Hambley, T. W.; Yau, B. C. K. *Inorg. Chem.* **1994**, *33*, 2009–2017.
(28) Smith, K.-T.; Tilset, M.; Kuhlman, R.; Caulton, K. G. *J. Am. Chem. Soc.* **1995**, *117*, 9473–9480.
(29) Sabo-Etienne, S.; Chaudret, B. *Coord. Chem. Rev.* **1998**, *178−180*, 381–407.

Table 3. NMR Data for *trans*-$[Ru(P_2)_2H(\eta^2\text{-}H_2)]^+$ Complexes[a]

complex	^{1}H NMR	^{31}P{^{1}H}	$J_{H\text{-}D}$, Hz	T_1(min), ms[b]	solvent
$[Ru(DHPrPE)_2H(H_2)]^+$ (**IIa**)[c]	−6.5 (s, br), −11.3 (q, $^2J_{P-H}$ = 20.1 Hz)	65.9	32	20.6 (500 MHz)	THF-d_8
$[Ru(DHMPE)_2H(H_2)]^+$ (**IIb**)[c]	−6.9 (s, br), −13.0 (q, $^2J_{P-H}$ = 19.7 Hz)	61.3	33	16.5 (500 MHz)	THF-d_8
$[Ru(DMeOPrPE)_2H(H_2)]^+$ (**IIc**)[c]	−6.6 (s, br), −11.4 (q, $^2J_{P-H}$ = 20.1 Hz)	63.4	32	21.1 (500 MHz)	THF-d_8
$[Ru(DEPE)_2H(H_2)]^+$ (**IId**)[26]	−6.4 (s, br), −11.3 (q, $^2J_{P-H}$ = 19.3 Hz)	60.8	32.0	16 (400 MHz)	acetone-d_6
$[Ru(DPPE)_2H(H_2)]^+$ (**IIe**)[26]	−4.6 (s, br), −10.0 (q, $^2J_{P-H}$ = 18 Hz)	68.6	32.9	20 (400 MHz)	acetone-d_6
$[Ru(DMPE)_2H(H_2)]^+$ (**IIf**)[27]	−7 (s, br), −13 (q, $^2J_{P-H}$ = 20.8 Hz)	40.3	32.2	16.1 (400 MHz)	ethanol-d_6

[a] DHPrPE = 1,2-bis(dihydroxypropylphosphino)ethane, DHMPE= 1,2-bis(dihydroxymethylphosphino)ethane, DMeOPrPE= 1,2-bis(dimethoxypropylphosphino)ethane, DEPE= 1,2-bis(diethylphosphino)ethane, DPPE= 1,2-bis(diphenylphosphino)ethane, DMPE= 1,2-bis(dimethylphosphino)ethane. [b] Spectrometer frequency (in MHz) listed in parentheses. [c] This work.

Scheme 1. Possible Pathways for the Heterolysis of H_2[a]

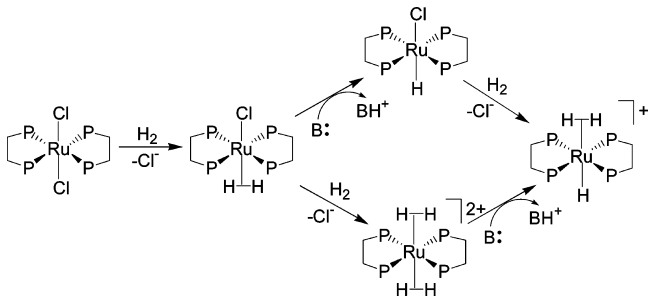

[a] In this scheme, B represents a generic base.

To investigate the mechanism of the formation of **II**, two key intermediates were synthesized by alternative routes using the DMeOPrPE ligand as the representative model for all the bidentate phosphines. One potential key intermediate, *trans*-$[Ru(DMeOPrPE)_2HCl]$, was prepared from $[Ru(COD)Cl_2]_n$, lithium hydroxide, and DMeOPrPE in refluxing methanol (eq 4).

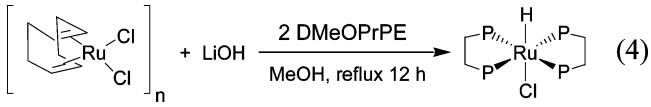

(4)

The complex exhibits a single resonance in the $^{31}P\{^1H\}$ spectrum at δ 59.1, suggestive of 4 equivalent phosphorus atoms, while the hydride region of the ^{1}H NMR spectrum gives rise to a quintet at δ −22.1 with a $^2J_{HP}$ of 20 Hz, consistent with *cis* P−H coupling (Figure 3).[30] When solutions of *trans*-$[Ru(DMeOPrPE)_2HCl]$ are treated at room temperature with 25 psig H_2, *trans*-$[Ru(DMeOPrPE)_2(H_2)H]^+$ forms within 5 min, as indicated by the appearance of a singlet at δ 63.4 in the $^{31}P\{^1H\}$ spectrum and the appearance of new resonances in the ^{1}H NMR spectrum for the *trans*-$[Ru(DMeOPrPE)_2(H_2)H]^+$ complex at −6.6 (s, br), −11.4 (q, $^2J_{P-H}$ = 20.1 Hz) (Table 3).

To test the viability of the bottom pathway in Scheme 1, the *trans*-$[Ru(DMeOPrPE)_2(H_2)Cl]^+$ was prepared and reacted with H_2. Specifically, when solutions of *trans*-$[Ru(DMeOPrPE)_2HCl]$ are treated with triflic acid (CF_3SO_3H), the singlet at δ 59.1 disappears and is replaced with another singlet at δ 49.9. Likewise, the quintet at δ −22.1 in the hydride region is replaced with a broad singlet (or alternatively, when CD_3OD is used as the solvent, a 1:1:1 triplet of triplets, representing the HD isotopologue) at δ −14.3. These data are consistent with assignment of the new species as *trans*-$[Ru(DMeOPrPE)_2(H_2)Cl]^+$ (Figure 4). The H−H bond distance was characterized by the T_1(min) value of 35.1 ms (500 mHz), consistent with an H−H distance of 0.94 Å (assuming fast rotation) or 1.18 Å (assuming slow rotation).[31,32] Furthermore, the $^1J_{HD}$ of 25.3 Hz is consistent with a distance of 1.00 Å based on Morris' correlation,[23] 1.01 Å for Heinekey's correlation,[24] and 1.03 Å using Gusev's correlation.[25] Such an increase in the H−H bond distance (compared to the *trans*-$[Ru(DMeOPrPE)_2(H_2)H]^+$ species) is consistent with the ability of a chloride ligand to act as a π-base and enhance electron donation to the σ^*-orbitals of the coordinated H_2, compared to a hydride ligand that can offer no such interaction. Addition of H_2 to a Et_2O/THF solution of *trans*-$[Ru(DMeOPrPE)_2(H_2)Cl]^+$, even in the presence of $TlPF_6$, did not lead to any reaction over a two week period, thus ruling out the bottom pathway in Scheme 1. Also when excess triflic acid was added to *trans*-$[Ru(DMeOPrPE)_2(H_2)H]^+$ no reaction was observed, again ruling out the bottom pathway.

In summary, the formation of *trans*-$[Ru(DMeOPrPE)_2(H_2)H]^+$ from *trans*-$[Ru(DMeOPrPE)_2HCl]$ demonstrates the viability of the top pathway in Scheme 1. Furthermore, the lack of reactivity of *trans*-$[Ru(DMeOPrPE)_2(H_2)Cl]^+$ toward H_2, even in the presence of a halide abstractor, strongly suggests that a *bis*-η^2-H_2 intermediate is unlikely under the reaction conditions used to generate the *trans*-$[Ru(DMeOPrPE)_2(H_2)H]^+$ complex.

Inertness to Substitution by Water. The dihydrogen complex **IIc** can be generated in non-polar organic solvents, as well as in water buffered at pH 7.[14] This intriguing observation led us to consider the reason why water did not displace an otherwise easily substitutable H_2 ligand. Accordingly, we sought to evaluate the generality of this phenomenon and to examine whether most complexes of the type *trans*-$Ru(P_2)_2(H_2)H^+$ are unreactive to water substitution. To our knowledge, there are only a few examples of H_2 complexes that are inert to water substitution in neat water,[17] and in the case of the $[Ru(H_2O)_5(H_2)]^{2+}$ complex, stability is only maintained when the solution is kept under a high pressure of H_2.[18,33]

Substitution Patterns of H_2. The unusual stability of complex **IIc** in water prompted an investigation to probe whether **IIc** is substitutionally inert in the presence of other

(30) See references in Table 3.

(31) Hamilton, D. G.; Crabtree, R. H. *J. Am. Chem. Soc.* **1988**, *110*, 4126–4133.
(32) Desrosiers, P. J.; Cai, L.; Lin, Z.; Richards, R.; Halpern, J. *J. Am. Chem. Soc.* **1991**, *113*, 4173–4184.
(33) Grundler, P. V.; Yazyev, O. V.; Aebischer, N.; Helm, L.; Laurenczy, G.; Merbach, A. E. *Inorg. Chim. Acta* **2006**, *359*, 1795–1806.

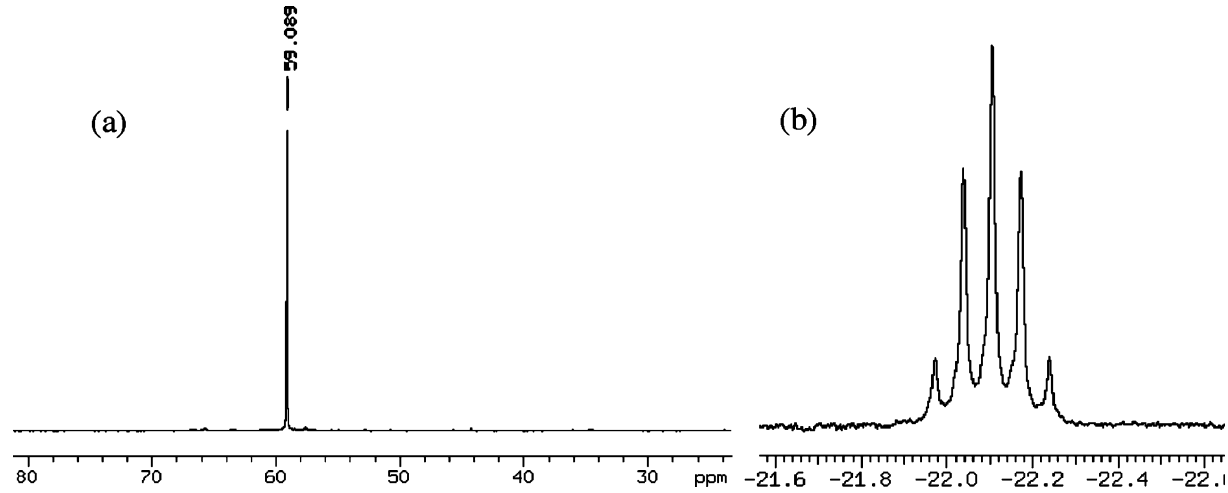

Figure 3. $^{31}P\{^1H\}$ NMR spectrum of (a) *trans*-$[Ru(DMeOPrPE)_2HCl$ and (b) the hydride region in the ^1H NMR spectrum (b).

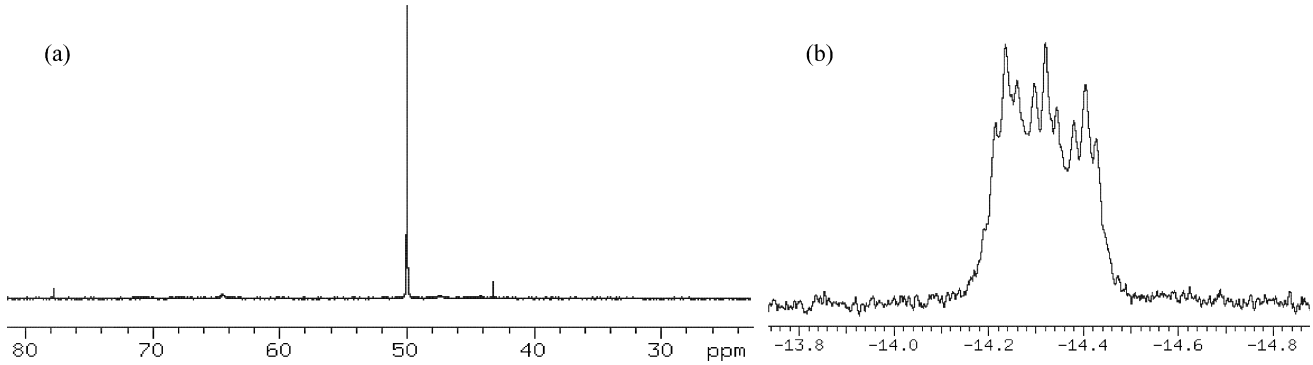

Figure 4. $^{31}P\{^1H\}$ NMR spectrum of (a) *trans*-$[Ru(DMeOPrPE)_2(H_2)Cl]^+$ and (b) the hydride region in the ^1H NMR spectrum of the HD isotopologue, *trans*-$[Ru(DMeOPrPE)_2(HD)Cl]^+$. The minor peak at δ 44.4 in spectrum (a) is unreacted *trans*-$Ru(DMeOPrPE)_2Cl_2$.

neutral ligands. It was thought that an examination of the ligand substitution patterns would lead to a better understanding of the reasons governing the substitutional inertness of the H_2 ligand in water. To probe the lability of the coordinated H_2 in the presence of a strong field ligand, the carbonyl complex *trans*-$[Ru(DMeOPrPE)_2H(CO)]^+$, was prepared by reacting *trans*-$[Ru(DMeOPrPE)_2(H_2)H]^+$ with CO. As reported previously, the reactions went to completion within minutes.[14]

While the reaction with CO confirms that the coordinated H_2 ligand can be easily substituted by a small, strong-field ligand, it was of interest to examine the effect that entering ligand size might have on the substitution of H_2 because of the steric constraints imposed by the chelating phosphine ligand. Restated, if the H_2 ligand is substitutionally inert in the presence of large entering ligands, this may be rationalized by the large methoxypropyl sidechains inhibiting substitution by physically protecting the coordinated H_2 from the entering ligand. Unexpectedly, it was found that substitution of the H_2 ligand was facile even with bulky ligands such as *tert*-butylnitrile and norbornadiene (see Supporting Information). The conclusion drawn from these substitution results is that the stability of the coordinated H_2 ligand cannot be understood solely from a steric standpoint, that is, the methoxypropyl arms of the DMeOPrPE ligand do not form a stabilizing pocket around the H_2.

Because the donor/acceptor properties of nitriles and olefins differ vastly from the purely σ-donating H_2O ligand, a substitution reaction with another σ-donating ligand, NH_3, was carried out. Substitution of H_2 by NH_3 in *trans*-$[Ru(DMeOPrPE)_2(H_2)H]^+$ (**IIc**) occurred within 10 min, as noted by the appearance of a new singlet at δ 58.6 (s) in the $^{31}P\{^1H\}$ NMR spectrum as well as a broad singlet at δ 0.18 (corresponding to the coordinated NH_3) and quintet at δ −20.1 (corresponding to the *trans* hydride) in the ^1H NMR spectrum,[34] concomitant with the disappearance of the starting material resonances. This result shows that the η^2-H_2 ligand can be easily substituted by a purely σ-donating ligand. Thus, the stability of the H_2 ligand toward substitution by water is not solely a consequence of the difference in donor/acceptor abilities. In summary of this section, the substitution reactions of coordinated H_2 in **IIc** were found to be facile for ligands of many sizes and donor abilities with the exception of H_2O.

Effect of Phosphine Donicity on H_2 Substitution. Because the $d_\pi-\sigma^*$ backbonding interaction is a crucial component that determines the strength of the $M-(H_2)$

(34) This NMR data is consistent with the DMPE analogue for which the crystal structure is known.[35]

(35) Fulton, J. R.; Sklenak, S.; Bouwkamp, M. W.; Bergman, R. G. *J. Am. Chem. Soc.* **2002**, *124*, 4722–4737.

Table 4. Infrared Carbonyl Bands (cm^{-1}) for *cis*-$P_2Mo(CO)_4$ Complexes

complex[a]	IR (CO) bands	solvent
(DHPrPE)Mo(CO)$_4$	2012, 1913, 1896	EtOH
(DEPE)Mo(CO)$_4$[38]	2012, 1909, 1891, 1873	DCE
(DMeOPrPE)Mo(CO)$_4$	2013, 1913, 1896	EtOH
(DMPE)Mo(CO)$_4$	2014, 1927, 1898, 1886	EtOH
(DHMPE)Mo(CO)$_4$	2018, 1926, 1901	EtOH
(DPPE)Mo(CO)$_4$	2020, 1915, 1892	EtOH

bond,[36,37] it was hypothesized that the coordinated H_2 ligand is stabilized by relatively electron-rich bidentate phosphine ligands. To probe this electronic effect, complexes bearing the same skeletal scaffold (*trans*-$[Ru(P_2)_2(H_2)H]^+$) with a variety of bidentate phosphine ligands were compared. Phosphines of varying donicities were selected. Initially, only water-soluble phosphines were selected because it was presumed they were required for the resulting H_2 complex to be soluble in water to discern the *aqueous* reactivity. However, the cationic nature of the *trans*-$Ru(P_2)_2(H_2)H^+$ complexes led to increased solubility in polar solvents, and complexes formed with non-water-solubilizing phosphines such as DMPE and DEPE were also found to have an appreciable solubility in water. To compare the relative electron-donating ability of the various phosphines used in the study, the highest energy $\nu(C{\equiv}O)$ band was compared in a series of substituted *cis*-$Mo(CO)_4P_2$ complexes (Table 4). The data are consistent with the well-known trend that the donor strength of the phosphine ligand is governed by the appending substituents.

Solutions containing *trans*-$Ru(P_2)_2(H_2)H^+$ (**IIa-f**) were treated with an excess of water (>100 equiv) to determine if the coordinated H_2 ligand would be substituted by water. Surprisingly, complexes **IIa**, **IIc**, **IId**, and **IIf** were unreactive to substitution by water (eq 5), even after a week at elevated temperatures (75 °C).

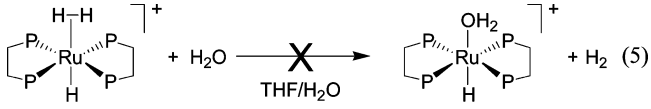

In contrast, complexes bearing DHMPE or DPPE ligands (**IIb**, **IIe**) were reactive toward substitution by water (eq 6). This was confirmed by the appearance of a new singlet in the ^{31}P NMR spectrum at δ 58.9 and δ 64.9 for **IIb** and **IIe**, respectively, as well as a crystal structure in the case of *trans*-$[Ru(DPPE)_2(H_2O)H]^+$ (Figure 5, Table 5).

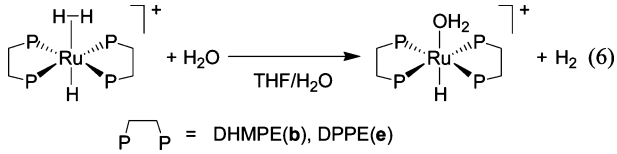

The substitution results can be explained by considering the inductive effects of the substituents appended to the phosphino ethane scaffold. The more electron donating

(36) Kubas, G. J. *Metal Dihydrogen and σ-Bond Complexes: Structure, Theory and Reactivity*; Kluwer Academic: New York, 2001.

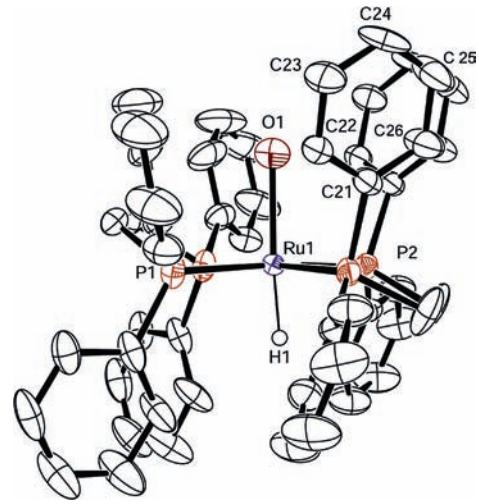

Figure 5. ORTEP representation of *trans*-$[Ru(DPPE)_2(H_2O)H]^+$. Ellipsoids are shown at 50% probability. Only the hydrogen atom bonded to the Ru atom is shown for clarity. The PF_6^- counterion is also omitted for clarity.

Table 5. Crystal Structure and Refinement Data for *trans*-$[Ru(DPPE)_2(H_2O)H]^+$

empirical formula	$C_{56}\ H_{51}\ F_6\ O_2\ P_5\ Ru$
formula weight	1125.89
temperature	173(2) K
wavelength	0.71073 Å
crystal system	orthorhombic
space group	*Pnma*
unit cell dimensions	a = 16.560(4) Å b = 19.896(5) Å c = 15.819(3) Å $\alpha = 90°$ $\beta = 90°$ $\gamma = 90°$
volume	5212(2) Å^3
Z, Z'	4, 0.5
density (calculated)	1.435 Mg/m^3
absorption coefficient	0.517 mm^{-1}
F(000)	2304
crystal size	0.17 × 0.07 × 0.04 mm^3
theta range for data collection	1.64 to 25.00°
index ranges	$-19 \le h \le 19$, $-17 \le k \le 23$, $-18 \le l \le 16$
reflections collected	26986
independent reflections	4734 [R(int) = 0.0783]
completeness to theta = 28.26°	100.0%
Absorption correction	semiempirical from equivalents
max. and min. transmission	0.9796 and 0.9172
refinement method	full-matrix least-squares on F^2
data/restraints/parameters	4734/6/301
goodness-of-fit on F^2	1.063
final R indices [I > 2sigma(I)]	R1 = 0.0660, wR2 = 0.1594
R indices (all data)	R1 = 0.0908, wR2 = 0.1724
largest diff. peak and hole	1.086 and −1.107 e Å^{-3}

phosphines (in **IIa**, **IIc**, **IId**, **IIf**) confer a more *inert* coordinated H_2 ligand because increased π-backbonding will occur to the H_2 ligand, which increases the Ru−H_2 bond energy. Conversely, when electron-withdrawing groups were appended to the phosphine backbone (**IIb**, **IIe**), the coordinated H_2 ligand was labilized with respect to substitution by water. The above results suggest that in *trans*-$Ru(P_2)_2(H_2)H^+$-type complexes, the energetics of H_2 coordination and H_2O coordination are similar and slight alterations in the electronics at the metal center can shift the favored complex. This thermodynamic explanation is consistent with the report by Kubas and co-workers who showed that the enthalpy of H_2

Table 6. Reaction Energies for Substitution of H_2[a]

reaction	reaction energy	reaction free energies[b]
$[Ru(DMPE)_2H(H_2)]^+ + H_2O$	0.46	0.82
$[Ru(DHMPE)_2H(H_2)]^+ + H_2O$	−0.13	−0.11
$[Ru(DMPE)_2H(H_2)]^+ + NH_3$	−4.63	−2.81
$[Ru(DMPE)_2H(H_2)]^+ + CO$	−22.97	−20.27

[a] Metal-ligand bond energies in kcal/mol. The reaction energies in the first column are simply the difference in SCF energies, without zero-point corrections or thermochemical corrections. [b] Including zero-point energy and thermochemical corrections at 373 K.

Table 7. Ru−L Bond Energies[a]

bond	bond energy	bond free energies[b]
$Ru-(H_2)$ in $[Ru(DHMPE)_2H(H_2)]^+$	15.37	2.04
$Ru-(H_2O)$ in$[Ru(DHMPE)_2H(H_2O)]^+$	15.50	2.14
$Ru-(H_2)$ in $[Ru(DMPE)_2H(H_2)]^+$	14.91	1.57
$Ru-(H_2O)$ in $[Ru(DMPE)_2H(H_2O)]^+$	14.45	0.75
$Ru-(NH_3)$ in $[Ru(DMPE)_2H(NH_3)]^+$	19.54	4.38
Ru−(CO) in $[Ru(DMPE)_2H(CO)]^+$	37.88	21.84

[a] Metal-ligand bond energies in kcal/mol. The bond energies in the first column are simply the difference in SCF energies, without zero-point corrections or thermochemical corrections. [b] Including zero-point energy and thermochemical corrections at 373 K.

binding was similar to H_2O in a tungsten carbonyl fragment, although in their case, the addition of excess water resulted in substitution of the H_2 ligand.[12]

An alternative explanation, based on kinetics, comes from transition-state theory. If a reacting M−L bond is strengthened, a higher activation barrier generally results, regardless of the energy of the products. Accordingly, a more highly donating phosphine ligand such as DEPE and DMeOPrPE will contribute to a higher activation barrier for ligand substitution. This may explain the lack of H_2O substitution in the case of the more electron-donating phosphine ligands.

Energetics of H_2 Coordination. To further examine the energetics of H_2 and H_2O coordination and the strength of the $Ru-H_2$ interaction, density functional theory (DFT) calculations were carried out. The two ruthenium phosphine complexes $[Ru(DHMPE)_2H(H_2)]^+$ (**IIb**) and $[Ru(DMPE)_2H(H_2)]^+$ (**IIf**) were chosen for the DFT studies because, experimentally, they have different reactivity toward substitution by water. The results of the calculations are shown in Tables 6 and 7. The reaction free energies, which include zero-point energy corrections and thermochemical corrections at the experimental temperature of 373 K, are at least qualitatively consistent with the experimental observations. Thus, for **IIf**, substitution of H_2 by H_2O was calculated to be slightly thermodynamically unfavorable, while substitution by NH_3 or CO was calculated to be thermodynamically favorable. For the **IIb** complex, substitution of H_2 by H_2O was calculated to be very slightly favorable. We do not expect the computed results to be quantitatively accurate because we have omitted solvation effects. Including solvation effects in this case is problematic for two reasons. First, most solvation models are based on a dielectric continuum, and these models have trouble modeling highly structured solvents like water unless they are heavily parametrized. Second, parametrized solvation models are generally developed for organic molecules, and the application of those models to charged organometallic complexes is questionable.

The calculated Ru−L bond free energies in Table 7 show that the $Ru-H_2$bond is very close in energy to the $Ru-H_2O$ bond for **IIb** and **IIf**, which explains why the reaction energies are essentially thermoneutral. The $Ru-NH_3$ bond in **IIf**, however, is calculated to be almost 3 kcal/mol stronger than the $Ru-H_2$ bond, and thus substitution of H_2 by NH_3 is predicted to be favorable. In summary, these calculations further support the fact that the $Ru-H_2$ and $Ru-H_2O$ complexes are energetically very similar, and alteration of the bidentate phosphine ligand can favor one complex or the other.

Conclusions

This study elucidated several key points to be considered when studying aqueous dihydrogen coordination chemistry. It was found that the reaction of *trans*-$[Ru(DMeOPrPE)_2Cl_2]$ with H_2 occurred by a stepwise H_2 addition/heterolysis pathway to yield a dihydrogen complex, *trans*-$[Ru(DMeOPrPE)_2(H_2)H]^+$. The resulting η^2-H_2 complex was surprisingly inert to substitution by water, even at concentrations as high as 55 M. The identity of the appended groups on the phosphine ligands influenced the lability of the coordinated η^2-H_2 ligand. With less donating phosphine ligands, the H_2 ligand was susceptible to substitution by H_2O, whereas with more electron-rich phosphine ligands, the H_2 ligand was *inert* to substitution by water. These results were substantiated by complementary DFT studies that showed the strengths of the $Ru-H_2$ and $Ru-H_2O$ bonds are quite similar in the $Ru(P_2)_2H^+$ fragment. The competitive binding ability of H_2 and H_2O for a group 8 transition metal has potential application in a number of areas.[39] Notably, a key step in the hydrogenase-mediated reduction of protons involves H_2 substitution for H_2O on an iron center.

Experimental Section

Materials and Reagents. Unless otherwise noted, all manipulations were carried out in either a Vacuum Atmospheres Co. glovebox (argon filled) or on a Schlenk line under argon or hydrogen using standard Schlenk techniques. The thallium hexafluorophosphate (**Caution!** *thallium compounds are toxic*), Proton Sponge, triflic acid, and lithium hydroxide were obtained from commercial vendors and used as received. 1,2-Bis(dihydroxypropylphosphino)ethane,[40] 1,2-bis(dihydroxymethylphosphino)ethane,[41] *trans*-$RuCl_2(DMeOPrPE)_2$ (**Ic**),[14] and $[RuCl_2(COD)]_n$[42] were prepared by published literature procedures. Reagent grade solvents were dried according to published procedures and deoxygenated with either an argon purge or three freeze-pump thaw cycles prior to use. Water was purified to a resistivity of 17−18 MΩ cm

(37) Maseras, F.; Lledos, A.; Clot, E.; Eisenstein, O. *Chem. Rev.* **2000**, *100*, 601–636.
(38) Chatt, J.; Watson, H. R. *J. Chem. Soc.* **1961**, 4980–4988.
(39) Szymczak, N. K.; Tyler, D. R. *Coord. Chem. Rev.* **2008**, *252*, 212–230.
(40) Baxley, G. T.; Weakley, T. J. R.; Miller, W. K.; Lyon, D. K.; Tyler, D. R. *J. Mol. Catal., A: Chem.* **1997**, *116*, 191–198.
(41) Nieckarz, G. F.; Weakley, T. J. R.; Miller, W. K.; Miller, B. E.; Lyon, D. K.; Tyler, D. R. *Inorg. Chem.* **1996**, *35*, 1721–1724.
(42) Albers, M. O.; Ashworth, T. V.; Oosthuizen, H. E.; Singleton, E. *Inorg. Synth.* **1989**, *26*, 68–77.

with a Barnstead Ultrapure system and was deoxygenated with an argon purge before use.

Instrumentation and Procedures. $^{31}P\{^1H\}$ and ^1H NMR spectra were recorded on a Varian Unity/Inova 500 spectrometer at an operating frequency of 500.62 (^1H) and 202.45 (^{31}P) MHz. The ^1H chemical shifts were referenced to an internal TMS standard and ^{31}P chemical shifts were referenced to an external standard of 1% H_3PO_4 in D_2O. Note that the ^1H NMR data for the methyl and methylene regions in complexes containing the DMeOPrPE ligand were generally broad and uninformative and therefore are not reported in the synthetic descriptions below. For spectra acquired at set temperatures, a 10 min temperature equilibration period was used. T_1 values were determined by plotting the intensity as a function of delay time and fitting the resultant curve to a 3-parameter single-exponential function. Unweighted Fourier transforms of each FID were phased carefully and subjected to baseline correction. When required, the samples were sealed under argon in 7 mm tubes fitted with Teflon valves. Mass spectra were obtained using an Agilent 1100 LC/MS Mass Spectrometer. The samples were dissolved in THF and introduced into the ionization head (ESI) using the infusion method. Elemental analyses were performed by Robertson Microlit Laboratories.

X-ray Crystallography. X-ray diffraction intensities were collected on a Bruker SMART APEX CCD diffractometer at $T =$ 153(2) K with Mo Kα radiation ($\lambda = 0.71073$ Å). The crystallographic data and summary of the data collection and structure refinement are given in Tables 2 and 5. Absorption correction was applied by SADABS.[43] The structures were solved using direct methods and completed by subsequent difference Fourier syntheses and refined by full matrix least-squares procedures on reflection intensities (F^2). All non-hydrogen atoms were refined with anisotropic displacement coefficients. Two $-CH_2-CH_2-$ groups in *trans*-$RuCl_2(DHMPE)_2$ (**Ia**), and one Ph-ring and PF_6 anion in *trans*-$[Ru(DPPE)_2(H_2O)H]^+$ are disordered over two positions in a 1:1 ratio. Only one position of the disordered atoms in these structures is drawn (Figures 2 and 5). The position of the H atom coordinated to the Ru atom in *trans*-$[Ru(DPPE)_2(H_2O)H]^+$ was found on the F-map and refined. Other H atoms were placed in calculated positions and were refined in a riding group model. The X-ray diffraction study of *trans*-$RuCl_2(DHPrPE)_2$ (**Ia**) showed that, in the crystal structure, there are two positions of the molecule, and as a result all atoms in the molecule (except the Ru atom) are disordered over two positions (Supporting Information, Figure S1). Our attempts to find a solution for this disorder and to further refine the structure failed. All software and sources scattering factors are contained in the SHELXTL (5.10) program package (G. Sheldrick, Bruker XRD, Madison, WI).

Computational Methods. All calculations were performed using Jaguar 6.5.[44] Geometry optimizations and the calculation of zero-point energies were carried out using the popular hybrid density functional known as B3LYP.[45,46] Thermochemical corrections to the energy were calculated at 373 K because that was the temperature used in the experimental studies of the substitution reactions. The basis set was LACV3P**. For the ruthenium atom, LACV3P** employs the quasi-relativistic Hay−Wadt pseudopotential[47] for the core electrons and the associated valence basis set contracted to triple-ζ form. For non-metals, LACV3P** employs the 6-311G** basis set.[48,49] Symmetry was not used for any of the calculations on the complexes.

Synthesis of *trans*-Ru(DHPrPE)$_2$Cl$_2$ (Ia). To a flask containing $RuCl_2COD$ (0.1871 g, 0.6679 mmol) was added a solution of DHPrPE (0.4412 g, 1.345 mmol) in ethanol (20 mL). After heating to reflux for 6 h, the solution was cloudy yellow. Upon cooling, a solid precipitate formed that was filtered and washed with hexanes (3 × 10 mL). The filtrate solvent was removed in vacuo, and the resulting solid was washed with hexanes (3 × 10 mL). A yellow solid was obtained. Yield: 0.33 g (59%). Crystals were obtained by cooling a saturated methanol solution in the freezer for 4 days. $^{31}P\{^1H\}$ NMR (CD_3OD): δ 41.2 (s). ^1H NMR (CD_3OD): δ 4.9 (s, 8H, -O*H*), 3.57 (t, 16H, CH_2OH), 2.17 (m, 16H, -CH_2-), 1.93 (m, 8H, PCH_2CH_2P), 1.85 (m, 16H, PCH_2-). $^{13}C\{^1H\}$ NMR (CD_3OD): δ 64.1 (-*C*H$_2$OH), 28.9 (-*C*H$_2$-), 22.9 (P*C*H$_2$CH$_2$P), 22.1 (P*C*H$_2$-). Anal. Calcd for $C_{28}H_{64}Cl_2O_8P_4Ru$: C, 40.78; H, 7.82; P, 15.02. Found: C, 41.19; H, 7.61; P, 15.05. **Id**, **Ie**, and **If** were synthesized by a similar procedure with the appropriate phosphine.

Synthesis of *trans*-Ru(DHMPE)$_2$Cl$_2$ (Ib). To a flask containing $RuCl_2COD$ (0.4617 g, 1.649 mmol) was added a solution of DHMPE (0.7062 g, 3.298 mmol) in ethanol (40 mL). After heating to reflux for 16 h, the solution was yellow with a brown/black solid lining the flask walls. The solution was filtered, the solvent was removed in vacuo, and the resulting solid was washed with petroleum ether (3 × 10 mL), followed by diethyl ether (3 × 10 mL), and tetrahydrofuran (3 × 10 mL). A yellow solid was obtained. Yield: 0.554 g (56%). Crystals were grown by cooling a saturated ethanol solution. $^{31}P\{^1H\}$ NMR (THF-d_8): δ 59.8 (s). ^1H NMR (THF-d_8): δ 4.4 (m, 8H, CH_2OH), 2.2 (m, 4H, -CH_2CH_2-), 1.9 (br s, 4H, -O*H*). $^{13}C\{^1H\}$ NMR (THF-d_8): δ 58.58 (*C*H$_2$OH), 18.88 (-*C*H$_2$CH$_2$-). Anal. Calcd for $C_{12}H_{32}Cl_2O_8P_4Ru$: C, 24.01; H, 5.37; P, 20.64. Found: C, 24.11; H, 5.34; P, 20.69.

General synthesis of *trans*-[Ru(P$_2$)$_2$(H$_2$)H]PF$_6$ (II-PF$_6$). To a stainless-steel pressure vessel containing *trans*-$Ru(DMeOPrPE)_2Cl_2$ (0.2843 g, 0.3037 mmol), $TlPF_6$ (0.2120 g, 0.6074 mmol), and Proton Sponge (0.0650 g, 0.3073 mmol) was added toluene (10 mL) and charged with H_2 (350 psig) and heated to 85 °C. After 16 h, the solution was cooled to room temperature and filtered through Celite in an argon-filled glovebox to yield a pale yellow solution. Following H/D exchange with CD_3OD, the HD isotopologue was visualized as a 1:1:1 triplet. Synthetic procedures that employed different phosphines were identical except that in the case of hydroxylated phosphines (DHMPE, DHPrPE), THF was used as the reaction solvent. These complexes were not isolated.

Synthesis of *trans*-Ru(DMeOPrPE)$_2$HCl. To a flask containing $RuCl_2COD$ (0.0721 g, 0.2567 mmol) and LiOH (0.013 g, 0.5417 mmol) was added a solution of DMeOPrPE (0.220 g, 0.5729 mmol) in methanol (20 mL). The solution was brought to reflux and within 30 min the cloudy brown solution turned transparent brown-red. Heating continued for 12 h, after which time solvent was removed in vacuo, then washed with boiling hexanes (3 × 10 mL), yielding a brown oil. Attempts to obtain a solid from the brown oil were unsuccessful. A $^{31}P\{^1H\}$ spectrum of the reaction mixture showed one major resonance at δ 59.1 (s). The ^1H NMR spectrum (CD_3OD) of the high-field region showed one resonance at δ −22.1 (quint., $^2J_{HP} = 21$ Hz). ESI+: *m*/*z* calcd for Ru(DMeOPrPE)$_2$H(Cl), 902.36. Found: $[M - H]^+$, 901.4.

Generation of *trans*-[Ru(DMeOPrPE)$_2$(H$_2$)Cl]$^+$. To an NMR tube containing a solution of *trans*-$[Ru(DMeOPrPE)_2HCl]$ (0.031 g, 0.034 mmol) in CD_3OD was added triflic acid (3 μL, 0.034 mol).

(43) Sheldrick, G. M. *SADABS (2.01), Bruker/Siemens Area Detector Absorption Correction Program*; Bruker AXS: Madison, WI.
(44) *Jaguar*, v6.5; Schrodinger, LLC: New York, 2005.
(45) Stephens, P. J.; Devlin, F. J.; Chabalowski, C. F.; Frisch, M. J. *J. Phys. Chem.* **1994**, *98*, 11623–11627.
(46) Becke, A. D. *J. Chem. Phys.* **1993**, *98*, 5648–5652.
(47) Hay, P. J.; Wadt, W. R. *J. Chem. Phys.* **1985**, *82*, 299–310.
(48) Krishnan, R.; Binkley, J. S.; Seeger, R.; Pople, A. J. *J. Chem. Phys.* **1980**, *72*, 650–654.
(49) McLean, A. D.; Chandler, S. G. *J. Chem. Phys.* **1980**, *72*, 5639–5648.

$^{31}P\{^{1}H\}$ NMR: δ 49.9 (s). ^{1}H NMR: δ −14.3 (1:1:1 tt; $^{1}J_{HD}$ = 25.3 Hz). T_1(min) = 35.05 ms (500 MHz). ESI+: *m*/*z* calcd for $[Ru(DMeOPrPE)_2(H_2)Cl]^+$, 903.37. Found: $[M - H_2]^+$, 901.4.

Acknowledgment. We thank the NSF for funding (NSF-CHE-0452004 and an NSF IGERT fellowship to N.K.S).

Supporting Information Available: ^{31}P NMR spectra of **I** and **II**, the crystallographic information including the.cif files and tables of bond lengths and angles of **Ib** and *trans*-$[Ru(DPPE)_2(H_2O)H]^+$, ball and stick representation of **Ia**, experimental procedures for the preparation of $Mo(P_2)(CO)_4$ complexes, experimental details for $[Ru(DMeOPrPE)_2(^tBuCN)H]^+$, $[Ru(DMeOPrPE)_2(C_7H_8)H]^+$, $[Ru(DMeOPrPE)_2(NH_3)H]^+$, $[Ru(DPPE)_2(H_2O)H]^+$, and $[Ru(DHMPE)_2(H_2O)H]^+$. This material is available free of charge via the Internet at http://pubs.acs.org.

IC801884X